

# The evolution of the hard X-ray luminosity function of AGN

James Aird

University of California, San Diego

Kirpal Nandra, Elise Laird, Antonis Georgakakis, Matt Ashby, Pauline Barmby, Alison Coil, Jiasheng Huang, Anton Koekemoer, Chuck Steidel, Chris Willmer

## Introduction

- The luminosity function of Active Galactic Nuclei (AGN) is a key tracer of the distribution and history of accretion activity over the lifetime of the Universe. Accurate measurements out to the highest possible redshifts are essential to constrain models of supermassive black hole formation and growth, the triggering and fueling of AGN, and their co-evolution with galaxies.
- X-ray surveys provide an efficient method of identifying AGN, including unobscured and moderately obscured sources, and low-luminosity AGN.
- However, a range of issues can lead to incompleteness in samples and potentially bias measurements of the X-ray luminosity function, especially at the faintest luminosities and highest redshifts.
- We present measurements of the 2–10 keV X-ray luminosity function (XLF) over a wide range of redshifts ( $z=0-3$ ).
- Use data from CDF-N (2Ms), CDF-S (2Ms), AEGIS-X (200ks), ASCA LSS and ASCA MSS
- We make a number of significant and important methodological improvements – see boxes 1–5
- We also present preliminary results from the AEGIS-XD (800ks) survey at  $z=4-5$

## 1) X-ray flux uncertainties and sensitivity

- Many X-ray sources detected with few counts  $\rightarrow$  significant Poissonian uncertainty in the flux
- We account for the full probability distribution for the flux of each source directly in our XLF fitting
- Also used in determination of the X-ray sensitivity function (see Georgakakis et al. 2008)
- Allows correction for the significant effects of Eddington bias (see Fig 1)

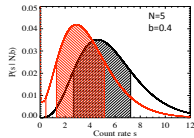


Fig. 1: Example Poisson probability distribution for X-ray count rate (black) and the distribution after correction for Eddington bias (red)

## 2) Correcting for incompleteness

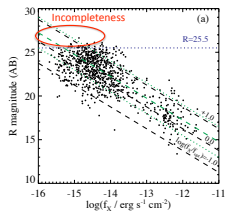


Fig. 2: X-ray flux vs. optical magnitude for our sample

- Likelihood Ratio (LR) method is used to identify secure optical counterparts of X-ray sources
- X-ray sources are scattered over a range of X-ray flux ratio
- For the faintest X-ray sources we suffer from incompleteness as sources lack optical counterparts
- Incompleteness is corrected for by directly modeling the  $f_x/f_{opt}$  relation in the determination of the XLF, and correcting for the fraction of sources with optical counterparts with  $R>25.5$

## 3) Photometric redshifts

- Photo-z essential to obtain adequate redshift completeness for low-luminosity AGN
- Adopt photo-z from CFHTLS (template fitting,  $u^*g^*r^*i^*z^*$ ) and ANNz (Artificial Neural Networks trained at  $z<1.2$ )
- Photo-z have large errors and there may be multiple peaks in the redshift probability distribution (see Fig. 3)
- $p(z)$  distributions are adopted for each source (see also box 5)
- Photo-z suffer from catastrophic failures and may be systematically biased at  $z>1.2$  (see Fig. 4). We therefore adopt an alternative approach at high redshifts (see box 4)

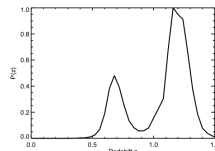


Fig. 3: Example redshift probability distribution,  $p(z)$ , for a CFHTLS photo-z

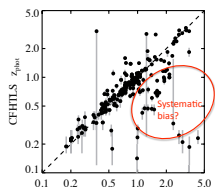


Fig. 4: CFHTLS photo-z vs. spectroscopic redshifts for AEGIS-X (200ks) sources

## 4) Rest-frame UV colour pre-selection at $z \approx 2-3$

- At  $z>1.2$  we restrict our sample to objects that satisfy rest-frame UV colour selection criteria in UGR colour space
- BX:  $z^*2.3$ , LBG  $z^*3$ , (Steidel et al. 2003, Adelberger et al. 2004)
- Such samples are highly incomplete
- However, have well-defined selection functions (see Fig. 6) that allow us to correct for this incompleteness
- Calculated by modeling colour distribution of different AGN hosts and simulating the observed data (see Fig. 5)

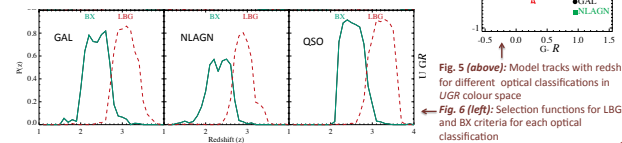


Fig. 5 (above): Model tracks with redshift for different optical classifications in UGR colour space

Fig. 6 (left): Selection functions for LBG and BX criteria for each optical classification

## 5) Bayesian model comparison

- Bayesian approach used to determine the XLF that accounts for the full probability distributions (i.e. uncertainties) in X-ray flux and redshift for each source, optical incompleteness, X-ray sensitivity and the high-z selection functions.
- Key feature: Bayesian evidence is calculated (via nested sampling algorithm), allowing robust model comparison - penalises more complex models
- Compare our luminosity and density evolution (LADE) with simpler Pure Luminosity Evolution (PLE) and more complex Luminosity-Dependent Evolution (LDDE)

## Conclusions

- Sophisticated method used to determine the evolution of the 2–10 keV XLF, which accounts for uncertainties in photometric redshifts, the Poissonian nature of X-ray flux estimates, the fraction of sources with counterparts below the magnitude limits of the optical data and the optical selection functions at high redshifts.
- We find that the XLF retains the same shape at all redshifts, evolving only in luminosity and overall density. There is no evidence for a flattening of the faint-end slope at high redshifts.
- The total luminosity density of AGN peaks at  $z=1.2 \pm 0.1$ , with a mild decline to higher redshifts. Lower luminosity AGN peak in number density at lower redshifts, but we find a smaller shift than prior studies.
- These results indicate that the same processes are responsible for triggering and fuelling AGN at all redshifts, but increase in overall density from the earliest times to  $z=1$ . Exhaustion of gas supplies in the most massive galaxies at later times may result in the “downsizing” of AGN to lower luminosities.
- We find that  $>50\%$  of black hole growth takes place at  $z>1$ , with around half in low-luminosity AGN.

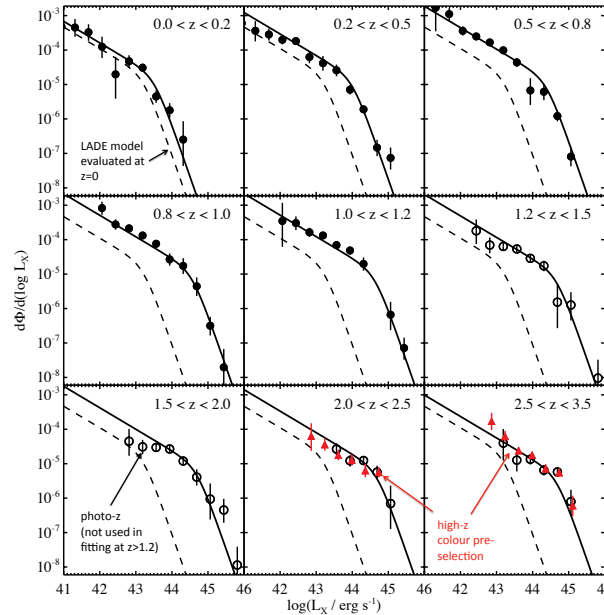
For more info see Aird et al. 2010, MNRAS, 401, 2531  
email: [jaird@ucsd.edu](mailto:jaird@ucsd.edu)

References: Adelberger K.L. et al., 2004, ApJ, 607, 226; Georgakakis A. et al., 2008, MNRAS, 388, 1205; Luo B. et al., 2010, ApJS, 187, 560; Steidel C.C. et al., 2003, ApJ, 592, 728

## Results

The XLF evolves in luminosity...

Moving to higher luminosities at higher redshifts  
This strong, positive evolution of the characteristic luminosity,  $L_c$ , dominates the evolution at  $z \leq 1.5$



... AND density  
Decreasing in overall density as redshift increases  
At high redshifts ( $z \geq 1.5$ ) the luminosity evolution slows, and the evolution is dominated by this weak exponential decline in density with increasing redshift.

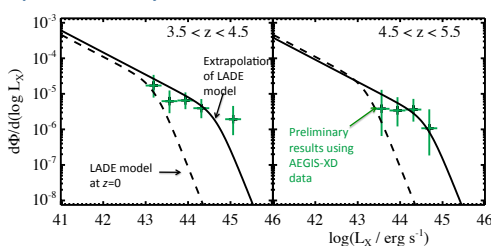
BUT retains the same shape

We find no evidence for a flattening of the faint-end slope at high redshifts. The XLF has the same shape at all redshifts. We do not require a more complex luminosity-dependent density evolution model (LDDE). Previous estimates may be biased by the failure of photometric redshifts at  $z=1.5-3$ , that can imply a flattened faint-end slope.

Fig. 7: 2-10 keV X-ray luminosity function at a range of redshifts

## The faint end of the XLF at $z \approx 4-5$ : preliminary results

- Additional 1.8 Ms of Chandra time awarded in A09 to take 3 of the AEGIS-X Chandra pointings to 800 ks depth – AEGIS-XD(eep)
- Provides a unique, large area of very deep X-ray data, providing a significant sample of low- $L_x$  AGN at  $z=4$
- X-ray sources are cross-identified with multiwavelength counterparts in optical, near- or mid-IR using the likelihood ratio technique  $\Rightarrow$  97% identification rate (see also Luo et al. 2010)
- Aperture magnitudes extracted for optically blank sources  $\Rightarrow$  upper limits
- Photo-z's determined from 10 bands from UV to 8.0  $\mu$ m



- Preliminary results agree well with extrapolation of LADE model

Fig. 8: Preliminary measurements of the 2-10 keV X-ray luminosity function at  $z=4$  and  $z=5$